Extending local magnitude ML to short distances

Richard Luckett[1], Lars Ottemöller [2], Antony Butcher[3] and Brian Baptie[1]

[1] *British Geological Survey, Edinburgh, EH14 4AP, UK.* *rrl@bgs.ac.uk*

[2] *University of Bergen, 5007 Bergen, Norway.*

[3] *University of Bristol, Bristol BS8 1RJ, UK.*

SUMMARY

Local magnitudes calculated at stations less than 10 km from earthquakes in the British Isles are up to one unit of magnitude higher than local magnitudes calculated at more distant stations. This causes a considerable overestimate of the event magnitude, particularly for small events, which are only recorded at short distances. Data from Central Italy and Norway shows that the same problem also occurs in other regions, suggesting that this is a more general issue for local magnitude scales. We investigate the addition of a new exponential term to the general form of the local magnitude scale. This corrects for the higher than expected amplitudes at short hypocentral distances. We find that the addition of this new term improves magnitude estimates in the three studied regions and magnitudes at short distances are no longer overestimated. This allows the use of a single scale that can be used at all distances, with a smooth transition between short and long distances. For the UK, the amended scale is $M_L = \log(amp) + 1.11 \log(r) + 0.00189r - 1.16e^{-0.2r} - 2.09$ and this is the scale now used by the British Geological Survey.

KEYWORDS

Earthquake ground motions, induced seismicity.

Robust estimation of earthquake magnitudes is essential when establishing a catalogue of seismic activity for seismic hazard assessments and other studies. The first magnitude scale was developed by Richter (1935) using observations of earthquakes in Southern California and is commonly referred to as the Local Magnitude, M_L. Despite the development of numerous other magnitude scales, M_L continues to be used in local and regional catalogues all around the world, often in its original form. This is the case in the UK, where the British Geological Survey (BGS) routinely estimates the size of local seismic events using the scale proposed by Richter (1935), as subsequently expressed by Hutton & Boore (1987). Intuitively, one would not expect it to be suitable for an intraplate region like the UK. Booth (2007), however, calculated distance-amplitude curves to show that the two regions are similar in this respect. This was confirmed by Ottemöller & Sargeant (2013), who used data from the UK to determine a new local magnitude scale that was essentially the same as Hutton & Boore (1987). Importantly, Ottemöller & Sargeant (2013) used almost no amplitudes recorded at less than 10km from the source.

More recently, 'traffic light systems' (e.g. Bommer et al., 2006; Majer et al., 2012) for the mitigation and management of induced seismicity in the geothermal and hydrocarbon industries can also use earthquake magnitude as a basis for modification or cessation of activities. Such control systems require robust and reliable estimation of event magnitudes in near real-time if they are to work effectively. Following the induced seismicity linked to fluid injection during hydraulic fracturing near Blackpool, UK, in 2011 (de Pater & Baisch, 2011), the UK Department for Energy and Climate Change published regulations (Department of Energy and Climate Change, 2013) that require hydraulic fracturing operations to stop if earthquakes with magnitudes of 0.5 M_L or greater are induced. Such events will only be detected by sensitive monitoring equipment near the epicentre. Since existing

networks of sensors in the UK are only able to reliably detect and locate earthquakes with magnitudes of 2.5 or greater, additional monitoring will be required to reliably detect and locate them.

Recent research has shown that amplitude measurements from epicentral distances of less than 15-20 km considerably overestimate magnitude compared to observations that are more distant. For example, magnitudes calculated for earthquakes induced by hydraulic fracturing at Preese Hall, Blackpool (Clarke et al., 2014), using ground motions recorded on seismometers a few kilometres away, were significantly higher than those magnitudes calculated using more distant observations. Butcher et al. (2017) found a similar problem for a sequence of mining events near New Ollerton, Nottinghamshire. Butcher et al. (2017) used this data to determine new constants for the M_L scale and suggested that this scale should be used when local monitoring networks are within 5 km of event epicentres. Strictly, this scale is only valid for data from the New Ollerton sequence. However, Butcher et al. (2017) showed that it gives reasonable results when applied to the earthquakes induced by hydraulic fracturing at Preese Hall. Additionally, the scale cannot be used above the suggested cut-off distance of 5 km, as it will result in incorrect estimates of magnitude. This cut-off distance is not well constrained, as no data at distances between 5 km and 50 km were used.

Clearly, this has important implications for a traffic light system based on a local magnitude threshold of 0.5. Earthquakes this small can generally only be recorded by stations very close to the source and using observations from distances less than 10-20 km will bias magnitudes to higher values. This will result in unnecessary cessation of activities, costly shutdown procedures and possible public alarm. If these problems are to be avoided, a new local magnitude scale is urgently required that can be applied at distances of a few kilometres to hundreds of kilometres.

In this paper, we examine the problem in detail. We show that, throughout the UK, individual station magnitudes within 5 km of an earthquake are up to one magnitude unit higher than station magnitudes at other stations. In many cases, this would cause a considerable increase in the event magnitude, beyond the magnitude expected from macroseismic information. We also use data from Central Italy and Norway to show that this is not only a problem in the UK. This suggests that this may be a more general issue for local magnitude scales. To address the problem, we suggest a modification to the general form of the local magnitude scale, with a new term to address higher than expected amplitudes at short hypocentral distances.. We use data from the UK, Central Italy and Norway to find appropriate values for new local magnitude scales that can be used to reliably calculate event magnitudes at all distances. We find that the form of the new scale generally improves magnitude estimates in each region and no longer results in overestimation of magnitude at short distances. This is relevant for all natural and induced seismicity, as any earthquake can occur very close to a seismic station, even if this is a relatively rare occurrence.

The challenge in introducing a new magnitude scale at the BGS is similar to that at many national networks. Previously calculated magnitudes have been widely distributed and it would be a major logistical effort to update the catalogue retrospectively. In any case, previous work has shown that the scale currently used is valid for earthquakes not recorded at nearby stations. Thus, one aim of the new scale is not to alter the magnitude for such earthquakes. It is, however, necessary to have a scale that is applicable to all earthquakes, whether they are recorded by such nearby stations or not. This is convenient and operationally helpful but the main reason is that individual earthquakes can be observed at stations at a range of distances. It is undesirable to calculate a single magnitude with two different scales, particularly because the precise distance where the transition should be made is not clear from the data available. Our motivation is to find a single scale that can be used at all distances with a smooth transition between short and long distances. The new scale documented

here satisfies both these requirements and will be routinely used by the BGS in the UK, including for traffic light systems for control of induced seismicity.

DATA

Great Britain

In 1969, the Institute of Geological Sciences (the predecessor of the BGS), installed the first modern seismometers in Britain, a network of eight stations in Central Scotland. Over the following decades this network grew in size, both in response to specific events, such as the Lleyn Peninsula earthquake in 1984 (Turbitt et al., 1985), and as a result of specific initiatives, such as monitoring North Sea seismicity. It reached a peak of 146 stations by the late nineties. Since then, the number of stations has been reduced to a permanent network of 80 stations, though temporary networks continue to be deployed to investigate aftershock sequences and possible induced seismicity. Data acquisition incorporates an event trigger and routine analysis of the resulting waveforms includes manual picking and association of phases, discrimination of event types and determination of locations and magnitudes. Origin, phase and waveform data for all seismic events are archived in a database that extends from 1969 to present and includes over 4500 earthquakes. These are published by BGS in the annual bulletins of earthquake activity (e.g. Galloway et al., 2013). Bulletin data are updated with revised parameter data published in BGS reports or peer-reviewed journal publications on specific earthquakes (e.g. Ottemöller et al., 2009). This catalogue is considered to be complete from 1979 onwards for all onshore earthquakes with local magnitudes of 2.5 or greater (Simpson, 2007). The earthquakes are located with a variety of velocity models depending on where they are in the UK (Booth et al., 2001).

A detailed examination of the BGS earthquake catalogue reveals an absence of amplitude data recorded at epicentral distances of less than a few kilometres. This can partly be explained by the high sensitivity and limited dynamic range of the instrumentation, which means that recordings at small epicentral distances were often saturated, even for modest magnitudes. However, even when the recordings remained on-scale, in many cases amplitudes were not included when calculating the magnitude. When the corresponding station magnitudes are calculated it becomes clear why. Station magnitudes for stations within 5 km of an earthquake tend to be higher than station magnitudes at more distant stations. In many cases, this would push the event magnitude up considerably – suggesting that they should have been felt when they were not. This has been of limited importance up to now because it happens so infrequently – fewer than 100 examples exist from the last four decades.

For this study, a detailed search of the database was made to find earthquakes that were recorded by an instrument within 20 km hypocentral distance. Only events recorded on more than five stations, with at least two of these more than 20 km away were accepted. The number of suitable events is reduced by the fact that, in many cases nearby stations were saturated. This is because, until the 21st century, the data telemetry for most stations limited the dynamic range to only 72 dB. A total of 82 suitable events are present in the database with 1049 amplitude observations with magnitudes ranging from 0.6 M_L to 3 M_L. This excludes the mining earthquakes at New Ollerton as explained below. These events are broadly distributed throughout the UK, occurring at a range of different depths, and their locations are shown in Fig. 1 alongside the distribution of amplitudes that contribute to their magnitude estimates.

It is interesting to look at the 82 events in slightly more detail. More than 100 earthquakes were recorded from a sequence of earthquakes in Manchester in late 2002 (Baptie & Ottemöller, 2003), many by three temporary, local stations installed by the BGS a few days after the sequence started.

Fourteen of these are included as they are large enough to be recorded at several distant stations but small enough not to saturate the nearby stations. A sequence of earthquakes in the Scottish Borders in 2004/2005 contributes a further nine events. No extra stations were deployed for this sequence, but the earthquakes occurred very close to a permanent station. In April 2011, a 2.3 M_L earthquake was induced by hydraulic fracturing of the first dedicated shale gas well in the UK, at Preese Hall near Blackpool (Clarke et al., 2014). The earthquake was felt by local people and caused considerable concern. In response, the BGS installed temporary seismometers very close to the drill site and recorded over fifty induced earthquakes, most of which were too small to be felt. Two of the largest, with local magnitudes of 1.3 M_L and 1.5 M_L, were also recorded by stations that are more distant and are included. In 1996/1997, two networks were deployed by the BGS to study mining induced seismicity in the Midland Valley of Scotland (Redmayne et al., 1998). These networks recorded hundreds of events, however, only one was recorded on distant stations without saturating the local stations. The remaining 56 earthquakes are located near stations throughout mainland UK.

An additional group of events in the BGS database is not included in its entirety, because there are so many events that it would bias any results. These are the earthquakes induced by mining at New Ollerton (Verdon et al., 2017). In February 2014, the BGS installed a network of seven seismometers around the mine after felt earthquakes in the vicinity. Unlike the similar deployments in Scotland two decades earlier, high dynamic range (120 dB) instruments were used and these never saturated. The network recorded over 300 earthquakes that followed the long-wall excavation of a seam at 900m depth. They were located with a velocity model published by Bishop et al. (1993). Many of these were clearly recorded on distant stations as well as the local network. However, because the source hardly moves many of the amplitude/distance data points are effectively repeated many times. Ten of the New Ollerton events are included in the dataset used in this work, meaning that there are a total of 92 earthquakes and 1253 amplitude observations.

The data used was recorded using a range of instruments over a significant time interval. Of the 1171 amplitudes recorded at permanent sites, 830 were recorded by modern broadband instruments. The instruments in these cases were either Guralp CMG-3T seismometers, with a corner frequency of 120 seconds, or Nanometrics Trillium seismometers, with a lower natural period of 240 seconds. 307 of the amplitudes were recorded on Willmore MkII short period seismometers with 1 Hz corner frequency. The short period acquisition, unlike that used later for the broadband stations, was susceptible to saturation, but none of the waveforms used in this data set were saturated. The remaining 38 amplitudes recorded at permanent sites were recorded by Integra 3JLA10 accelerometers. These were collocated with seismometers and have been used here when the accompanying short period instrument saturated. The temporary deployments at New Ollerton and Blackpool make up the remaining 78 amplitudes. These were recorded on Guralp CMG-3ESP seismometers with a 30 second corner frequency. In all cases, the sampling frequency was 100 Hz. All the sites used have been shown to measure the expected amplitudes for distant earthquakes, ruling out any site or instrument effects from our calculations. For example, a 3.1 M_L earthquake occurred near Oakham in Rutland on 17th April 2014 and was recorded on 19 stations, including those at New Ollerton, 60 km away. The magnitudes calculated for the four New Ollerton stations were 3.1, 3.0, 3.0 and 3.0.

Fig. 2 shows the difference between station magnitude and event magnitude for the earthquakes in this dataset. Each data point marks the average of all the residuals calculated at that hypocentral distance (rounded down to the nearest km) and averages are only plotted for distances with more than three observations. The error bars show one standard deviation. Station magnitudes clearly increase for stations less than around 10 km from an earthquake and may be as high as one magnitude unit higher than station magnitudes at more distant stations. In many cases, this would push the event magnitude up considerably, beyond the magnitude expected from macroseismic

information. The abnormally large residuals at 57 km and 58 km in this plot are an artefact caused by having a localised cluster of 10 earthquakes (the New Ollerton events). These earthquakes were recorded on a station known, over many years, for recording lower amplitudes than expected for earthquakes at all distances. This station is 57 km from the mine. There is only one other data point at this distance, meaning that the site effect of the single station creates the observed glitch.

The BGS follow Hutton & Boore (1987) and only measure amplitudes on the horizontal components. This is done using the SEISAN earthquake analysis package (Havskov & Ottemöller, 1999). Simulated Wood–Anderson seismograph readings are produced by removing the actual instrument response and convolving with the response of an instrument with a period of 0.8 s and a damping factor of 0.8. A gain of 2080 (Uhrhammer & Collins, 1990) is added to produce the same units as the Wood–Anderson instrument used by Richter (1935).

Amatrice

On 24th August 2016, a 6 Mw earthquake struck near Amatrice in central Italy, causing many fatalities and heavy damage (Pucci et al., 2017). About two weeks later the BGS, in cooperation with the Istituto Nazionale di Geofisica e Vulcanologia (INGV) and Edinburgh University deployed a temporary network of 24 three-component, broadband sensors to record aftershocks and study the evolution of the sequence (Moretti et al., 2016). The instruments used were Guralp CMG-6T seismometers with a corner frequency of 30 seconds, sampled at 100 Hz. Thousands of aftershocks were recorded by this network in September and October 2016 and the high station density resulted in numerous recordings at distances of less than 10 km. Nearly all of these events occurred at depths less than 10 km (Chiaraluce et al., 2017). The location of the earthquakes, alongside the distribution of amplitudes that contribute to their magnitude estimates are shown in Fig. 3.In order to reduce the huge number of earthquakes to a manageable number only those events close to several stations are chosen. All those used have at least one observation with a hypocentral distance of less

than 10 km, at least 5 observations with hypocentral distances of less than 20 km and at least 5 observations with hypocentral distances greater than 20 km. This results in 12045 observations from 287 earthquakes. Fig. 4 is similar to Fig. 2 and shows the difference between station magnitude and event magnitude. Again, station magnitudes clearly increase for stations less than around 10 km from an earthquake. Magnitudes in this dataset range from 0.4 M_L to 4.1 M_L. Having so much data allowed us to test the robustness of the inversion. Magnitudes were calculated for this data using the same scale as for the UK (Hutton & Boore, 1987), as this is reported by Amato & Mele (2008) as the scale used by the INGV. It is interesting that Amato & Mele also report that the INGV routinely discard amplitudes recorded closer than 30 km from an earthquake, as using them results in overestimating the magnitude. A more recent M_L scale for Italy has been developed by Di Bona (2015), but that was not used for this deployment and does not address the issue of measurement at short distances.

Northern Norway

The coastal stretch of Northern Norway roughly between Mo i Rana and Bodø is among the more seismically active areas in Norway. The largest historic earthquake in mainland Norway of 5.8 M_L occurred here in 1819 (Bungum, 2005). Swarm-like activity is a typical feature of this intraplate area, such as the Meløy swarm in 1978 (Bungum & Husebye, 1979). We use data from the NEONOR2 temporary experiment that covered the area with 27 seismometers, in addition to five permanent stations of the Norwegian National Seismic Network (NNSN), between 2013 and 2016. The seismometers used were Guralp CMG-3ESP and Streckeisen STS2.5 broadband seismometers with corner frequencies of 60 seconds and 120 seconds respectively. They were sampled at 100 Hz. During this time, starting in April 2016 an earthquake swarm occurred near Jektvik. Including only earthquakes with amplitudes measured at more than five stations, at least one of which is closer than 20 km, we were able to use 617 earthquakes with M_L between -0.4 and 3.3 with 6664

amplitudes. The location of the earthquakes, alongside the distribution of amplitudes that contribute to their magnitude estimates are shown in Fig. 5. Fig. 6 is equivalent to Fig. 2 and Fig. 4 and shows the difference between station magnitude and event magnitude. As for the UK and the Amatrice sequence data, station magnitudes clearly increase for stations less than around 10 km from an earthquake.

M_L is routinely calculated by the NNSN using the scale developed for Norway by Alsaker et al. (1991). In contrast to the UK, amplitude measurements are done on the vertical channel, but otherwise the routine of calculating magnitudes is the same. Inspecting the data showed that the problem of over-estimating M_L at short distances is similar to the UK although slightly less severe.

ANALYSIS

The first magnitude scale was developed by Richter (1935) to standardise the description of earthquake size. He defined an earthquake as 3 M_L if it caused the pen of a Wood–Anderson seismograph to move 1 mm at a station 100 km away. He produced a table of corrections so that the same earthquake had the same magnitude at all distances. Subsequently, Bakun & Joyner (1984) suggested replacing the tabulated values for the amp_0 factor by an attenuation curve described in terms of distance and log of distance by

$$M_L = \log(amp) - A \log\left(\frac{r}{100}\right) + B \log(r - 100) + S + 3 \qquad (1)$$

Where *amp* is the amplitude at a given station, *r* is the hypocentral distance to the earthquake and *S* is a station correction. The constants *A, B* and *S* were found by performing a least squares fit to California data. Different values of *A* and *B* are appropriate in different places (e.g. Kiratzi and Papazachos, 1984, Alsaker et al., 1991, Ristau et al., 2016) and extra terms have been added in some

regions to improve consistency (Uhrhammer et al., 2011). In the UK, the station correction, S, is not used and the values for A and B found by Hutton & Boore (1987) are used, as shown to be appropriate by Booth (2007). The equation used by the BGS is:

$$M_L = \log(amp) + 1.11 \log(r) + 0.00189r - 2.09 \tag{2}$$

In which amp is the displacement amplitude in nanometres and r is the hypocentral distance in kilometres (Ottemöller & Sargeant, 2013). Ottemöller & Sargeant (2013) inverted for new values of A and B using UK data and found the relation

$$M_L = \log(amp) + 1.06 \log(r) + 0.00182r - 1.98 \tag{3}$$

Adopting a new scale would require the BGS to recalculate and republish the entire catalogue and the change implied by the new relationship was considered to be small enough to make that unnecessary. Ottemöller & Sargeant (2013) achieved a better result if station corrections were applied. In practice, however, as data accumulates the best value for individual station corrections changes – this results in a constantly changing scale that is not suitable for routine analysis.

To avoid changing the existing catalogue it was decided to fix the values of A and B to those in equation 2. A term is then required that only applies to amplitudes recorded at short hypocentral distances. This will only affect the few events described above in the data section. Visual examination of the data shown in Figs 2, 3 and 4 shows that amplitudes decay rapidly in the distance range 0-20 km, suggesting that an additional exponential term can be used to account for this. Adding the exponential term De^{-Er} to the scale, we get:

$$M_L = \log(amp) - A\log\left(\frac{r}{100}\right) + B\log(r - 100) + De^{-Er} + 3 \tag{4}$$

In theory, there should also be a term $-De^{-E100}$ to ensure that Richter's definition is satisfied, but this is insignificant for all the values of E considered. Each set of data is assembled into a system of linear equations:

$$-\log(amp_{ij}) = A\log(r_{ij}) + Br_{ij} + De^{-Er_{ij}} - M_{Li} + C \qquad (5)$$

Where M_{Li} is the average magnitude for event i and C is a constant that ensures the condition that an amplitude of 481 nm (1 mm on a Wood-Anderson seismograph with a gain of 2080) will give a magnitude of 3 at 100 km (Richter, 1935). Singular value decomposition (SVD, Menke, 1989) is used to optimise C, D and M_{Li} for fixed values of A and B. The parameter E was changed in a grid search with values between 0.0 and 0.5 with an increment of 0.1, while inverting for D using the SVD. The values adopted for each data set were those that produced the lowest root-mean-square residual, as defined by

$$RMS = \sqrt{\frac{1}{N}\sum_{ij}(M_{Lij} - M_{Li})^2} \qquad (6)$$

Where N is the number of amplitude observations.

RESULTS

The three data sets were treated separately and each optimised for D and E in Equation 5. In all cases, the values for A and B were fixed. The value for C, responsible for ensuring a magnitude 3 at 100 km, did not change, as the new term is negligible at that distance. For all three sets of

earthquakes, the RMS residual was reduced by the addition of the new term (Table 1). The shape of

the M_L distance correction, –logA0 (Hutton & Boore, 1987) in each case is shown in Fig. 7.

The changes in residual in Table 1 are small because most of the station magnitudes remain the

same. Only station magnitudes close to the earthquake change at all. However, the changes to these

station magnitudes are appreciable and bring them much closer to the average magnitude for the

event. This can be seen in Fig. 8, which shows the same data as Figs 2, 4 and 6 after application of

the new scale. The distance at which the new term acts varies between the regions studied. In the

UK, the values of D and E mean that magnitude measurements beyond 12 km will be altered by less

than 0.1. For Amatrice the equivalent distance is 20 km and for the NEONOR2 data, it is 22 km. The

Amatrice dataset is large enough that it allowed us to test the robustness of the inversion. A less

strictly selected subset of 627 earthquakes (as opposed to the 287 used above) resulted in D and E

values less than 10% different from those presented here. This corresponds to a difference in the

new term much less than 0.1 at a distance of 2 km. An additional sensitivity test was carried out

using the UK data. Ten sets of 80 earthquakes were selected randomly from the 92 earthquakes

used above. The same method was applied and the results compared with those for the whole

dataset. The value of E varied between 0.19 and 0.21 (compared with 0.20 for all the data). The

value of D varied between -1.12 and -1.18 (compared with -1.16). The maximum corresponding

change to the new term is 0.01 at a distance of 2 km.

An effort was made to show the statistical significance of the decrease in RMS residual, as the RMS

will always decrease if an extra term is added. This was done by bootstrapping with resampled

residuals. The station magnitude residuals for each event in the UK dataset were randomly

reallocated to other channels with a magnitude for that event. This was done by converting the

magnitude residuals to amplitude residuals, assuming that equation 3 gives the real magnitude. The

amplitude residual was then removed from each pick and replaced with a randomly chosen (without

replacement) residual from the same event. The inversion process described above was then carried out exactly as for the original data and the RMS noted. The residual reallocation and inversion process was repeated 1000 times and in 98% of the runs the RMS with the new term found was greater than that for the real data with the new term from Table 1. This is taken to mean that the decrease in RMS from using the new term is statistically significant at the p=0.05 level.

As an illustration, the two largest earthquakes induced by hydraulic fracturing operations in May 2011 at Preese Hall, Blackpool, with local magnitudes of 1.3 and 1.5 ML, were analysed with the new scale. These events were recorded by a local station (BHHF) at a distance of 1.5 km, as well as by a number of regional stations in the distance range 70-200 km. For the event at 22:35 on the 26th May 2011, the amplitudes recorded at BHHF would, using the standard BGS scale, correspond to a magnitude of 2.2 M_L. This is much higher than the average magnitude of 1.3 M_L calculated for the other five stations. With the new scale, the station magnitude decreases to 1.6 M_L. Similarly, for the earthquake at 00:48 on the 27th May. The station magnitude for BHHF changes from 2.5 M_L to 1.9 M_L compared with an average at the other six stations of 1.5 M_L. This puts the magnitudes recorded at BHHF within the range of values observed at the other stations. Fig. 9 shows how the event magnitude changes for all events in the three datasets when the new formula is used. For most events, the event magnitude does not change, as there are no stations very close or the single station magnitude affected does not change enough to change the average.

DISCUSSION AND CONCLUSION

The local magnitude scale incorporates corrections for geometrical spreading and anelastic attenuation. These are dependent on both the structure and elastic properties of the Earth, through which the seismic waves have travelled. The form of Equation 1 was chosen by Bakun and Joyner (1984) so that the first term accounts for geometrical spreading at a rate of r^A and the second term

accounts for anelastic attenuation with coefficient B proportional to $1/Q$, where Q is known as the quality factor. However, these terms are found empirically by inverting amplitude data and often the best fitting individual terms are such that any physical interpretation is inappropriate. An example of this is a scale recently optimised for New Zealand earthquakes (Ristau et al., 2016), where the geometric spreading term of 1.27×10^{-03} cannot be explained physically. These numbers are empirical and need not have physical significance for the scale to work.

The over-estimation of the station magnitude based on the standard scale at short distances tells us that the amplitudes are greater relative to the simple M_L formula and its attenuation model. This is arguably no surprise as $-log A0$ changes the most toward shorter distances and at the same time there is often no constraint based on data. Geometrical spreading cannot be used to explain the observed increase in amplitudes at short distances, as it has been shown to have a stronger effect near to the source – thereby reducing amplitudes, rather than increasing them. Studies indicate that geometrical spreading causes amplitudes to decrease at a rate of approximately $1/r^{1.4}$ within the first 20km, rather than the $1/r$ rate typically seen at greater distances (e.g. Wu et al., 2016). This means that assuming constant geometric spreading over all distances, as in the standard equation, will cause an underestimate of magnitude at these distances. The fact that an overestimate as is observed, means that another factor is more than compensating for any effect of geometrical spreading.

Similarly, the observed effect cannot be explained by lower attenuation at near-source distances. Numerous studies (e.g. Edwards et al., 2008) have shown that the quality factor, Q, which is inversely proportional to the anelastic attenuation, is generally expected to increase as a function of depth. As a result, the effect of attenuation is expected to be greater at sites close to shallow sources, since most of the ray path is in the highly attenuating near surface. Amplitudes at short

hypocentral distances (which implies a shallow source) would have reduced amplitudes compared to those expected by assuming constant attenuation.

One explanation for amplitudes greater than those predicted using standard attenuation relationships is that a different phase is being measured. This would imply a different path and different attenuation to the phases tabulated by Richter. At distances less than about 120km (Edwards et al., 2011) the phase with the highest amplitude is normally Sg/Lg. The attenuation of this phase will be that accounted for when inverting for $-logA0$. However, Fig. 10 shows that at the shortest distances Sg is small in amplitude compared to a later arrival. As an illustration, in Fig. 10 the amplitudes of Sg for NOLA and NOLE – the two closest stations – would give station magnitudes 1.1 and 1.2 less than the actual station magnitude and in both cases would be equal to the corresponding event magnitudes. The group velocity of this phase increases with distance from the source as shown in Fig. 11.

There is evidence that high frequency surface waves become an important part of the waveform at distances less than 20 km for shallow sources (Myers et al., 1999). These surface waves have larger amplitudes than Sg, but attenuate quickly, particularly if there are heterogeneities in near-surface geology. They will therefore determine M_L at short distances, but be unimportant at larger distances. The frequency observed by Meyers et al. (4-5 Hz) is the same as the frequency of the highest amplitude parts of the near-source waveforms here. However, looking at particle motion plots of the highest amplitude part of near-source waveforms does not indicate that surface waves are being observed directly. Myers et al (1999) invoked Rg to S scattering to explain the amplitudes they observed close to explosions in a deep borehole. Rg amplitude is very dependent on depth (Ma & Motazedian, 2012) but the hypocentral distance criteria used to select events for this study mean that events are almost all less than 10 km deep with the vast majority less than 5 km deep, making them strong sources for Rg. There is insufficient data to try to uncouple depth and hypocentral

distance with this dataset. High amplitude surface wave energy, that is only present at short

distances for shallow earthquakes, is a working hypothesis for why the new term is necessary.

The best way to explain the observed discrepancy is that Richter's original work on local magnitude

did not include sufficient near-source data. As a result, the scale does not properly represent

observations at these distances. The addition of an exponential term to the M_L scale, allows us to

correct for higher than expected amplitudes at small epicentral distances. This applies to the three

regions that we investigated. The basic observations for the respective regions are the same, despite

differences in the near-surface geology requiring corresponding correction terms.

The form of the extra term was chosen simply because it describes the observed data. The

underlying physical reason is not clearly understood. Other authors (e.g. Chavez & Priestley, 1985;

Butcher et al., 2017) have suggested using different ML scales for different distance ranges.

However, the scale presented here can be used to calculate earthquake magnitude at a wide range

of distances and avoids the need to define a transition distance. For earthquakes only recorded at

distances greater than about 20 km (which is the vast majority of earthquakes recorded in the UK),

the magnitude will be the same as that calculated using the current BGS scale. For earthquakes

recorded partly or solely by stations closer than about 10 km the magnitude will be lower than that

calculated with the current scale. This will be the correct magnitude for these events and there will

be much less scatter between near and far stations where both are present.

The addition of an exponential term to the local magnitude scale improves magnitude estimates in

the three studied regions and stops the overestimation of magnitude at short distances. The new

scale can be used at all distances with a smooth transition between short and long distances. The

BGS is now using the exponential term when calculating magnitudes for UK earthquakes. This means

that the equation now used is:

$$M_L = \log(amp) + 1.11 \log(r) + 0.00189r - 1.16e^{-0.2r} - 2.09 \tag{7}$$

REFERENCES

Alsaker, A., Kvamme, L., Hansen, R., Dahle, A. & Bungum, H., 1991. The ML scale in Norway, *Bull. Seismol. Soc. Am.*, **81**, 379–398.

Amato, A. & Mele, F., 2008. Performance of the INGV National Seismic Network from 1997 to 2007, *Annals of Geophysics*, **51**, 417-431, doi:10.4401/ag-4454.

Bakun, W. & Joyner, W.B., 1984. The ML scale in central California, *Bull. Seismol. Soc. Am.*, **74**, 1827–1843.

Bishop, I., Styles, P. & Allen, M., 1993. Mining-induced seismicity in the Nottinghamshire Coalfield, *Quarterly Journal of Engineering Geology*, **26**, 253-279.

Baptie, B. & Ottemöller, L., 2003. The Manchester earthquake swarm of October 2002, *EGS - AGU - EUG Joint Assembly, Abstracts from the meeting held in Nice, France, 6 - 11 April 2003*, abstract #10286

Bommer, J., Oates, S., Cepeda, J., Lindholm, C., Bird, J., Torres, R., Marroquín, G. & Rivas, J., 2006. Control of hazard due to seismicity induced by a hot fractured rock geothermal project, *Eng. Geol.,* **83**(4):287–306.

Booth, D., Bott, J. & O'Mongain, A., 2001. The UK Seismic velocity model for earthquake location – a baseline review, *British Geological Survey Internal Report*, IR/01/188. 20pp.

Booth, D, 2007. An improved UK local magnitude scale from analysis of shear and *Lg*-wave amplitudes, *Geophys. J. Int.,* **169**, 593–601.

Bungum, H., 2005. The 31st of August 1819 Lurøy earthquake revisited, *Norsk Geologisk Tidsskrift*, **85**, 245-252.

Bungum, H. & Husebye, E., 1979. The Meløy, northern Norway, earthquake sequence - a unique intraplate phenomenon, *Norsk Geologisk Tidsskrift*, **2**, 189-193.

Butcher, A., Luckett, R., Verdon, J., Kendall, M., Baptie, B. & Wookey, J., 2017. Local Magnitude Discrepancies for Near-Event Receivers: Implications for the U.K. Traffic-Light Scheme, *Bull. Seismol. Soc. Am.*, **107**, doi: 10.1785/0120160225

Chávez, D. E. & Priestley, K. F., 1985. ML observations in the Great Basin and M0 versus ML relationships for the 1980 Mammoth Lakes, California, earthquake sequence, *Bull. Seismol. Soc. Am*., **75**, 1583–1598.

Chiaraluce L., Di Stefano, R., Tinti, E., Scognamiglio, L., Michele, M., Casarotti, E., Cattaneo, M., De Gori, P., Chiarabba, C., Monachesi, G., Lombardi, A., Valoroso, L., Latorre, D., Marzorati, S., 2017. The 2016 Central Italy Seismic Sequence: A First Look at the Mainshocks, Aftershocks, and Source Models, Seismol*. Res. Lett*., **88,** doi: 10.1785/0220160221

Clarke, H., Eisner, L., Styles, P. & Turner, P., 2014. Felt seismicity associated with shale gas hydraulic fracturing: The first documented example in Europe, *Geophys. Res. Lett.,* **41**, 8308–8314, doi:10.1002/2014GL062047.

de Pater, C. & Baisch, S., 2011. Geomechanical Study of Bowland Shale Seismicity. Cuadrilla Resources Ltd Available at http://energyspeakswv.com/Resources/Docs/Studies/Final_Report_Bowland_Seismicity_02-11-11.pdf (accessed 19/04/ 2017).

Department of Energy and Climate Change, 2015. Onshore Oil and Gas Exploration in the UK: Regulation and Best Practice, Department of Energy and Climate Change, London, England.

Di Bona, M., 2016. A Local Magnitude Scale for Crustal Earthquakes in Italy, *Bull. Seismol. Soc. Am*. **106**, 242-258, doi: 10.1785/0120150155.

Edwards, B., Rietbrock, A., Bommer, J. & Baptie, B., 2008. The Acquisition of Source, Path, and Site Effects from Microearthquake Recordings Using Q Tomography: Application to the United Kingdom, *Bull. Seismol. Soc. Am*, **98**, 1915–1935, doi: 10.1785/0120070127.

Edwards, B., Fäh, D. & Giardini, D., 2011. Attenuation of Seismic Shear Wave energy in Switzerland, *Geophys. J. Int.,* **185**, 967–984, doi: 10.1111/j.1365.

Galloway, D., 2013. Bulletin of British Earthquakes 2012. *British Geological Survey Report*, OR/13/054.

Havskov, J. & Ottemoller, L., 1999. SeisAn Earthquake analysis software, *Seis. Res. Lett*., **70,** 532-534**.**

Hutton, L. K. & Boore, D. M., 1987. The ML scale in southern California, *Bull. Seismol. Soc. Am*. **77**, 2074–2094.

Kiratzi, A. & Papazachos, B., 1984. Magnitude scales for earthquakes in Greece. *Bull. Seismol. Soc. Am*. **74**, 969-985.

Ma, S. & Motazedian D., 2012. Depth determination of small shallow earthquakes in eastern Canada from maximum power Rg/Sg spectral ratio, *J. Seismol*., **16**, doi:10.1007/s10950-011-9252-9

Majer, E., Nelson, J., Robertson-Tait, A., Savy J. & Wong, I., 2012. Protocol for Induced Seismicity Associated with Enhanced Geothermal Systems. DOE/EE-0662.

Menke, W., 1989. Geophysical Data Analysis: Discrete Inverse Theory, *Int. Geophys. Ser*. Vol. 45, Academic, San Diego, California

Myers, S., Walter, W., Mayeda, K. & Glenn, L., 1999. Observations in Support of Rg Scattering as a Source for Explosion S Waves: Regional and Local Recordings of the 1997 Kazakhstan Depth of Burial Experiment. *Bull. Seismol. Soc. Am*. **89**, 544-549.

Moretti, M. et al., 2016. SISMIKO: emergency network deployment and data sharing for the 2016 central Italy seismic sequence, *Annals of Geophysics*. **59**, doi:10.4401/ag-7212.

Ottemöller, L., Baptie, B. & Smith, N., 2009. Source parameters for the 28 April 2007 Mw 4.0 earthquake in Folkestone, United Kingdom. *Bull. Seismol. Soc. Am*., **99** (3). 1853-1867

Ottemöller, L., & Sargeant, S., 2013. A local magnitude scale ML for the United Kingdom. *Bull. Seismol. Soc. Am*. **103**, 2884–2893.

Pucci, S., et al., 2017. Coseismic ruptures of the 24 August 2016, Mw6.0 Amatrice earthquake (central Italy), *Geophys. Res. Lett*., **44**, doi:10.1002/2016GL071859.

Redmayne, D., Richards, J. & Wild, P., 1998. Mining-induced earthquakes monitored during pit closure in the Midlothian Coalfield. *The Quarterly Journal of Engineering Geology* **31**, Part 1: 21-36

Richter, C. F., 1935. An instrumental earthquake magnitude scale, *Bull. Seismol. Soc. Am*. **25**, 1–32.

Ristau, J., Harte, D. & Salichon, J., 2016. A Revised Local Magnitude (ML) Scale for New Zealand Earthquakes. *Bull. Seismol. Soc. Am*. **106**, doi: 10.1785/0120150293.

Simpson, B.A., 2007. Bulletin of British Earthquakes 2006, *British Geological Survey Internal Report*, OR/07/003.

Turbittt, T., Barker, E., Browitt, C., Howells, M., Marrow, P., Musson, R., Newmark, R., Redmayne, D., Walker, A., Jacob, A., Ryan E. & Ward, V., 1985. The North Wales earthquake of 19 July 1984, *J. Geol. Soc.*, *London*, **142**, 567-71.

Uhrhammer, R.A. & Collins, E.R., 1990. Synthesis of Wood–Anderson seismograms from broadband digital records. *Bull. Seismol. Soc. Am*. **80**, 702–716.

Uhrhammer, R. A., Hellweg, M., Hutton, K., Lombard, P., Walters, A., Hauksson, E. & Oppenheimer, D., 2011. California Integrated Seismic Network (CISN) Local Magnitude Determination in California and Vicinity. *Bull. Seismol. Soc. Am*. **101**, doi:10.1785/0120100106.

Verdon, J., Kendall, M., Butcher, A., Luckett, R. & Baptie, B., 2017. Seismicity Induced by Longwall Coal Mining at the Thoresby Colliery, Nottinghamshire, U.K., *Geophys. J. Int.,* ggx465, https://doi.org/10.1093/gji/ggx465.

Wu, Q., Chapman, M., Beale, J. & Shamsalsadati, S., 2016. Near-Source Geometrical Spreading in the Central Virginia Seismic Zone Determined from the Aftershocks of the 2011 Mineral, Virginia, Earthquake, *Bull. Seismol. Soc. Am*., **106**, doi:10.1785/0120150314.

	A	B	C	RMS	D	E	RMS
UK	1.11	0.00185	-2.09	0.33	-1.16	0.2	0.28
Amatrice	1.11	0.00185	-2.09	0.32	-3.05	0.17	0.27
Northern Norway	0.91	0.00087	-1.67	0.25	-0.74	0.09	0.22

Table 1. Original values for *A, B* and *C* used in each region followed by the RMS for the current

dataset using the standard M_L equation. The optimum values found in this work for D and E are then

given with the new RMS obtained when adding the new term to the magnitude equation.
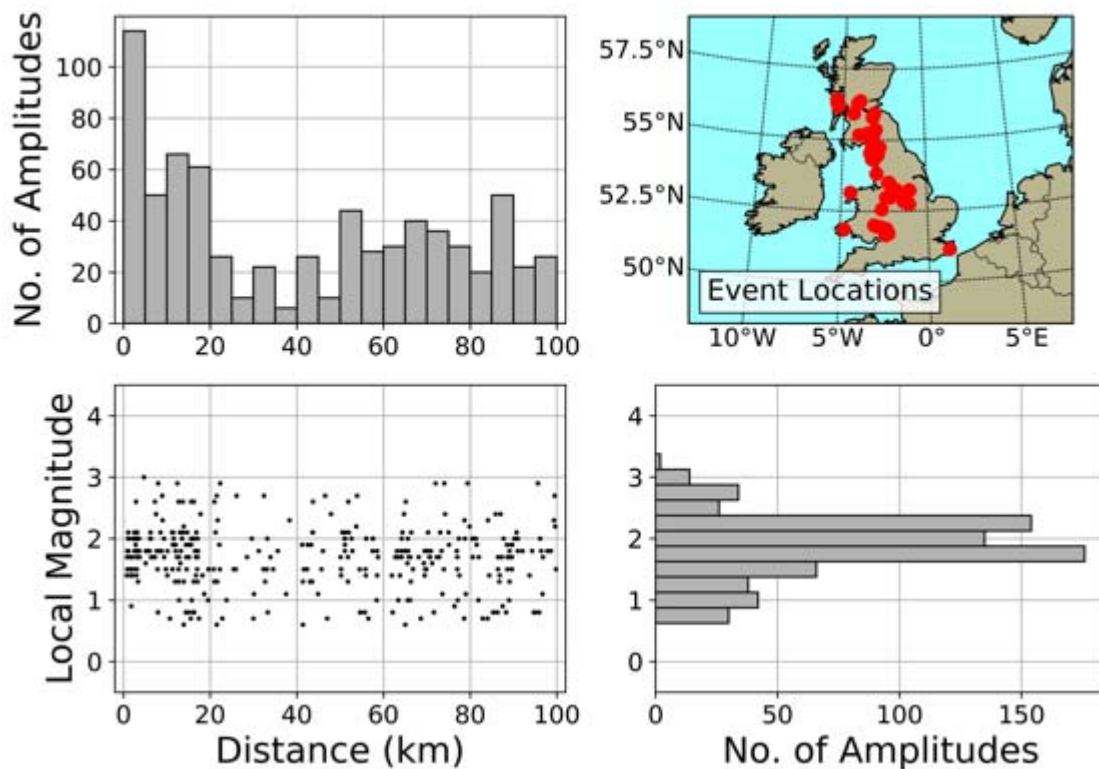
Figure 1. Magnitude and hypocentral distance distribution of the amplitudes comprising the UK dataset. Mgnitudes are those calculated using the method described in this paper. The map shows the location of the earthquakes used.
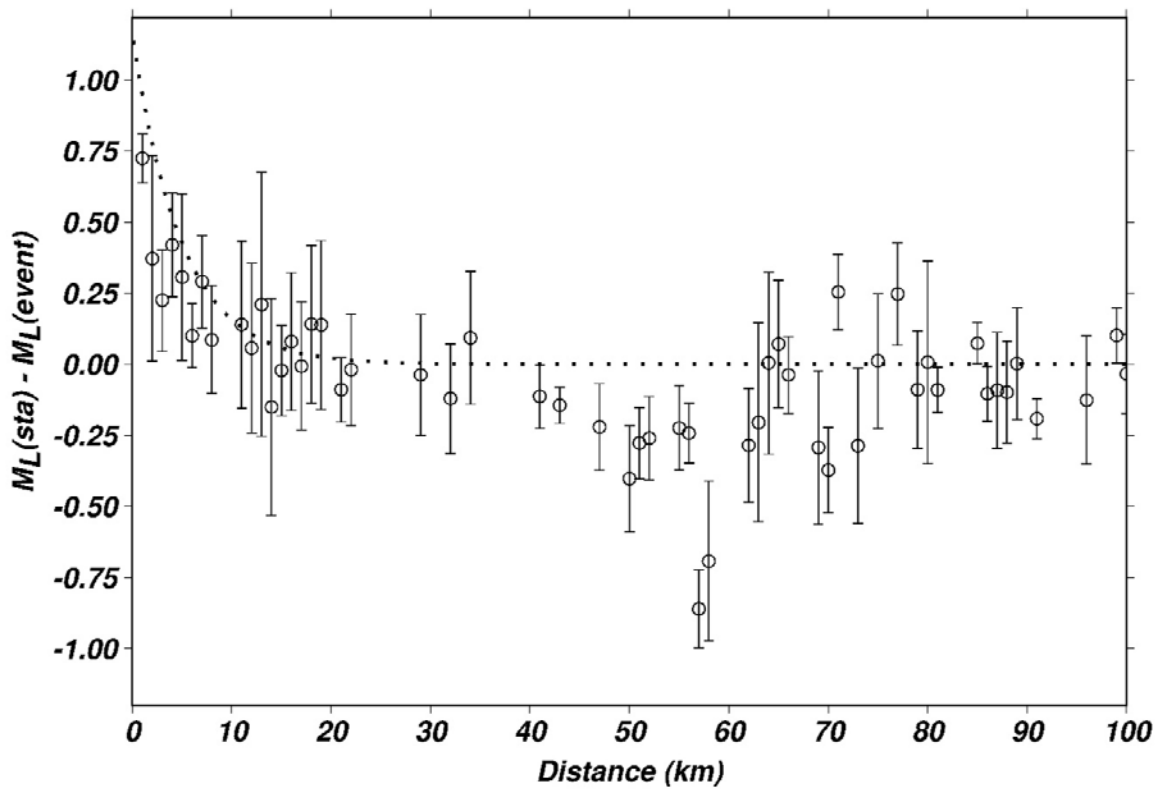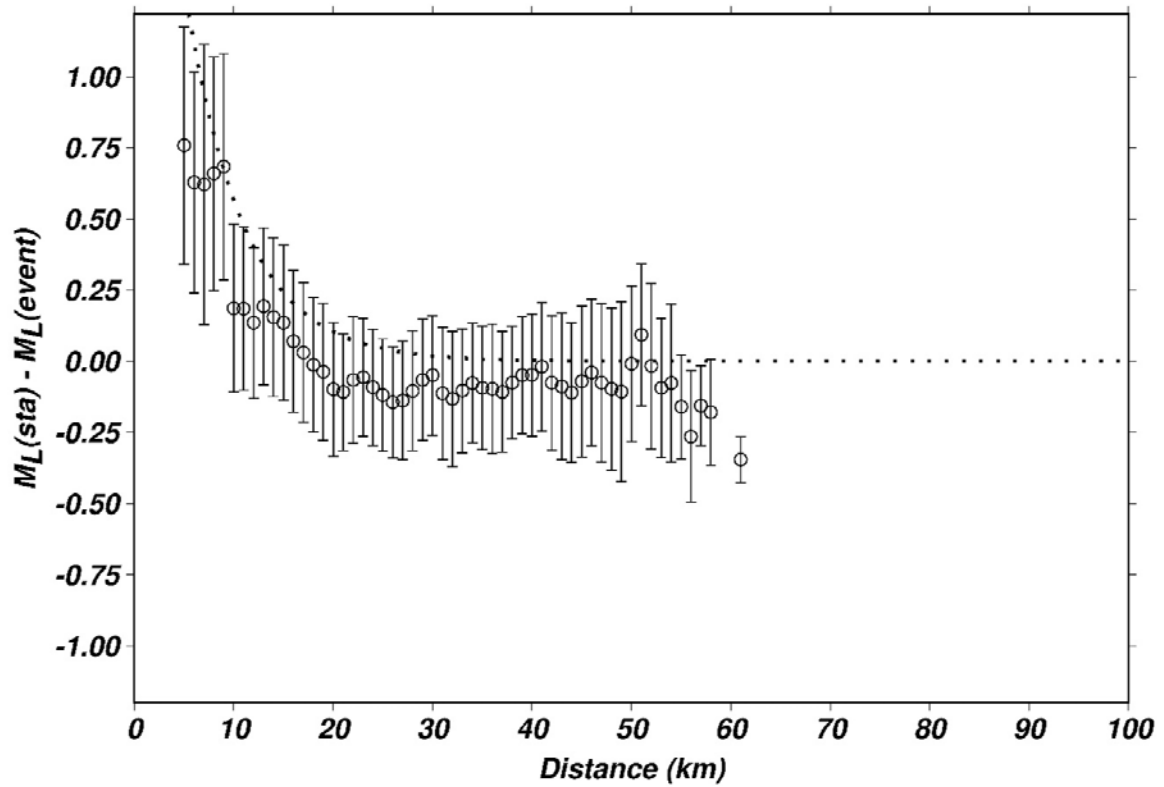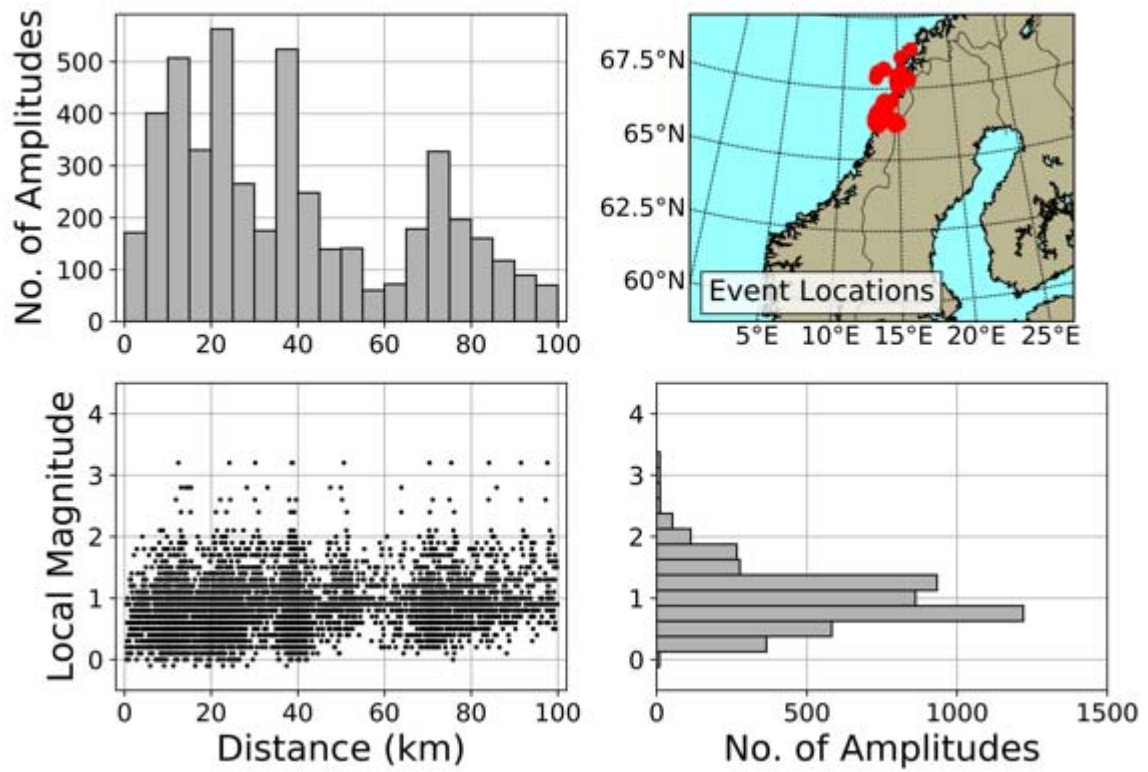

Figure 2.   Residuals between station magnitude and event magnitude for the 92 earthquakes selected from the BGS catalogue. Each data point marks the average of all the residuals calculated at that hypocentral distance. Averages are only plotted for distances with more than three observations and the error bars show one standard deviation. The dotted line is the value of $1.16\, e^{-0.2\, r}$, as explained in following parts of the paper.
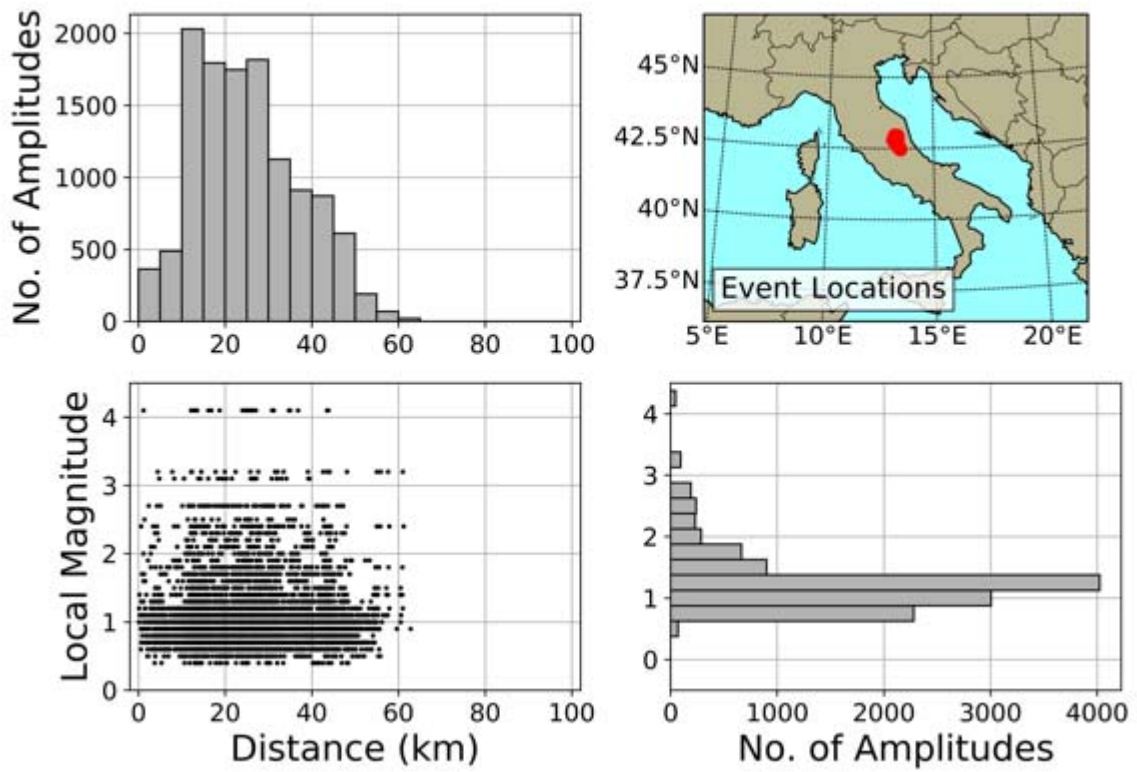
Figure 3. Magnitude and hypocentral distance distribution of the amplitudes comprising the Amatrice dataset. Mgnitudes are those calculated using the method described in this paper. The map shows the location of the earthquakes used.
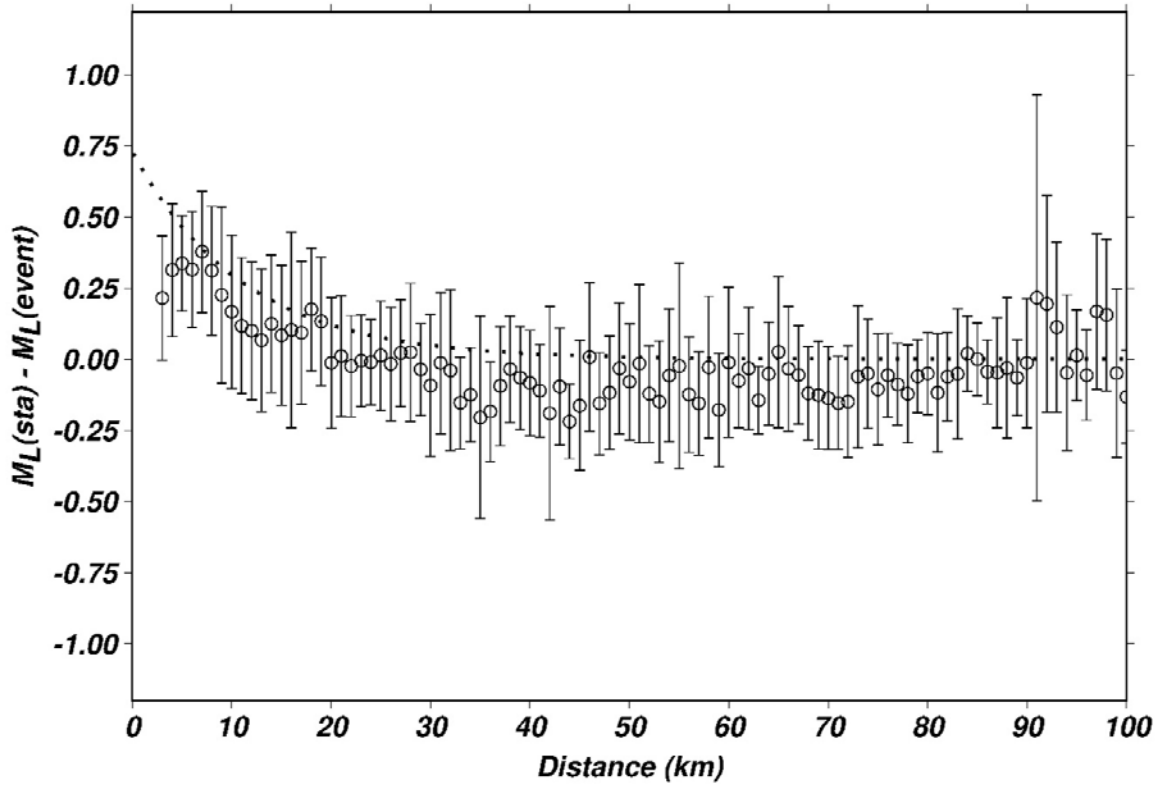
Figure 4. Residuals between station magnitude and event magnitude for the 287 earthquakes selected from the Amatrice dataset. Each data point marks the average of all the residuals calculated at that hypocentral distance. Averages are only plotted for distances with more than three observations and the error bars show one standard deviation. The dotted line is the value of $3.1\,e^{-0.17r}$, as explained in following parts of the paper.

Figure 5. Magnitude and hypocentral distance distribution of the amplitudes comprising the

NEONOR2 dataset. Mgnitudes are those calculated using the method described in this paper. The

map shows the location of the earthquakes used.

Figure 6. Residuals between station magnitude and event magnitude for the 617 earthquakes selected from the NEONOR2 dataset. Each data point marks the average of all the residuals calculated at that hypocentral distance. Averages are only plotted for distances with more than three observations and the error bars show one standard deviation. The dotted line is the value of $0.74\,e^{-0.09\,r}$, as explained in following parts of the paper.
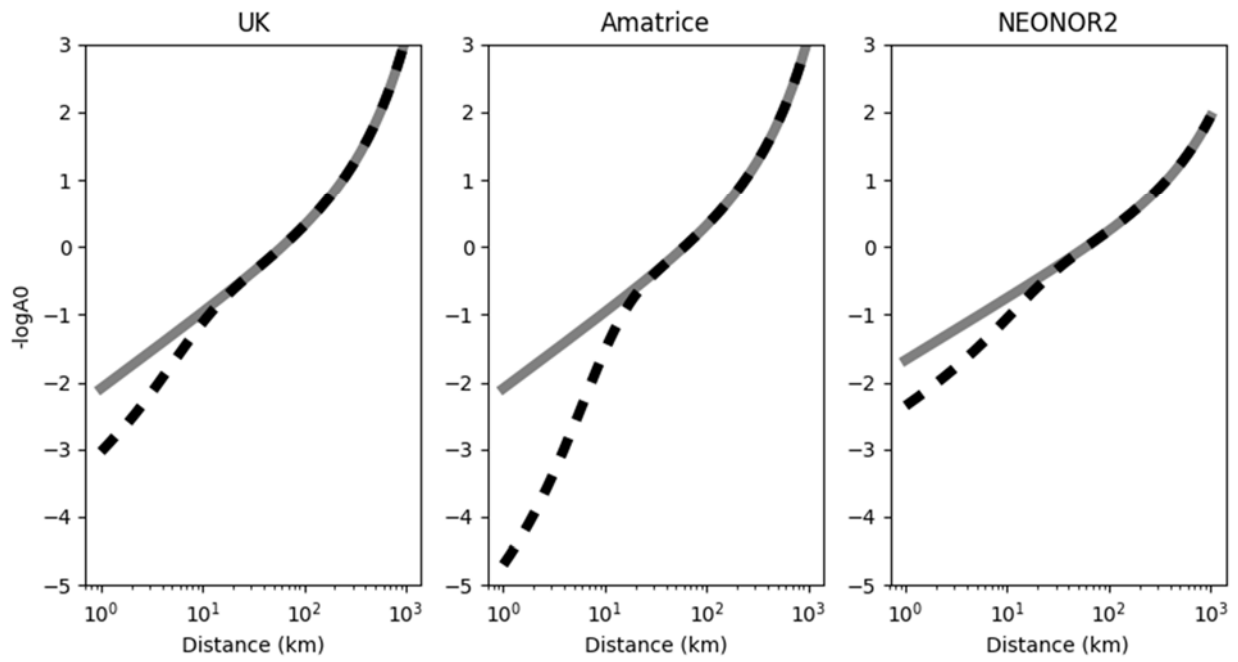
Figure 7. The attenuation correction term –logA0 shown for the three scales discussed here. In each case, the solid line is for the unaltered scale and the dotted line is for the scale including the new term.
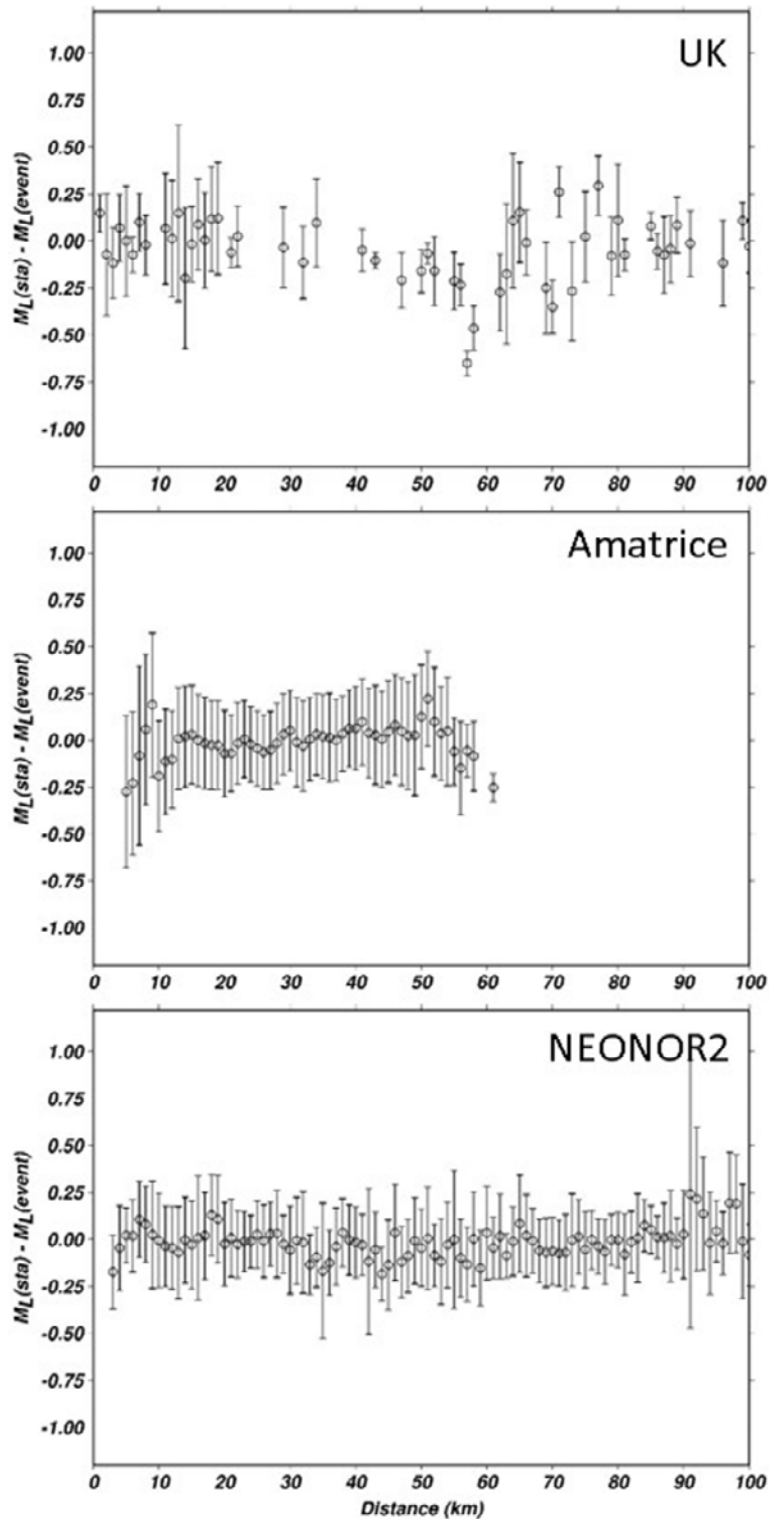
Figure 8. Residuals between station magnitude and event magnitude for three datasets after inclusion of the new term. Each data point marks the average of all the residuals calculated at that hypocentral distance. Averages are only plotted for distances with more than three observations and the error bars show one standard deviation.
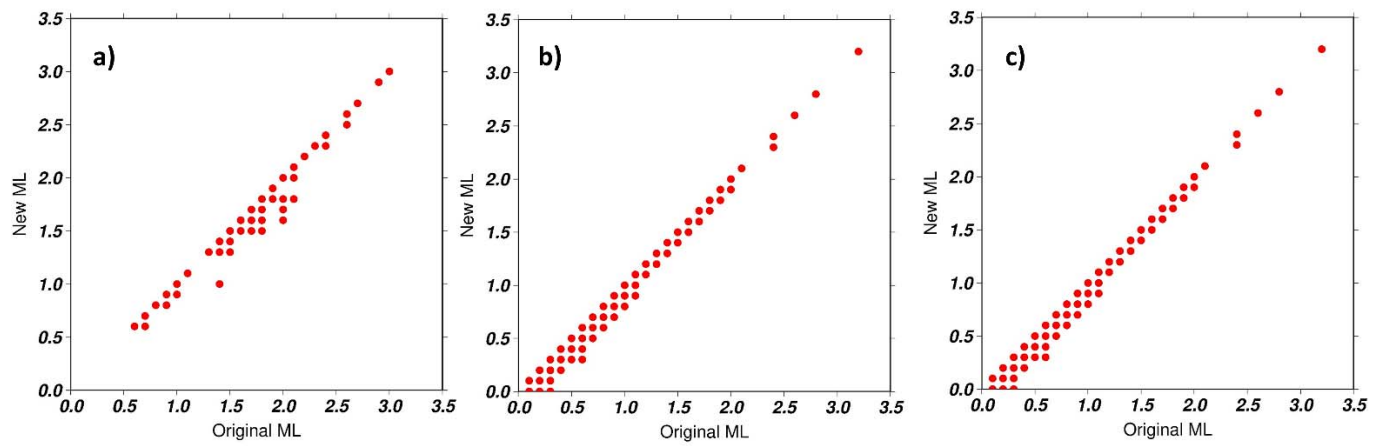
Figure 9. Event magnitudes for the three datasets before and after the correction has been applied. Many events have no stations close enough to be affected by the new term and so the event magnitude does not change.
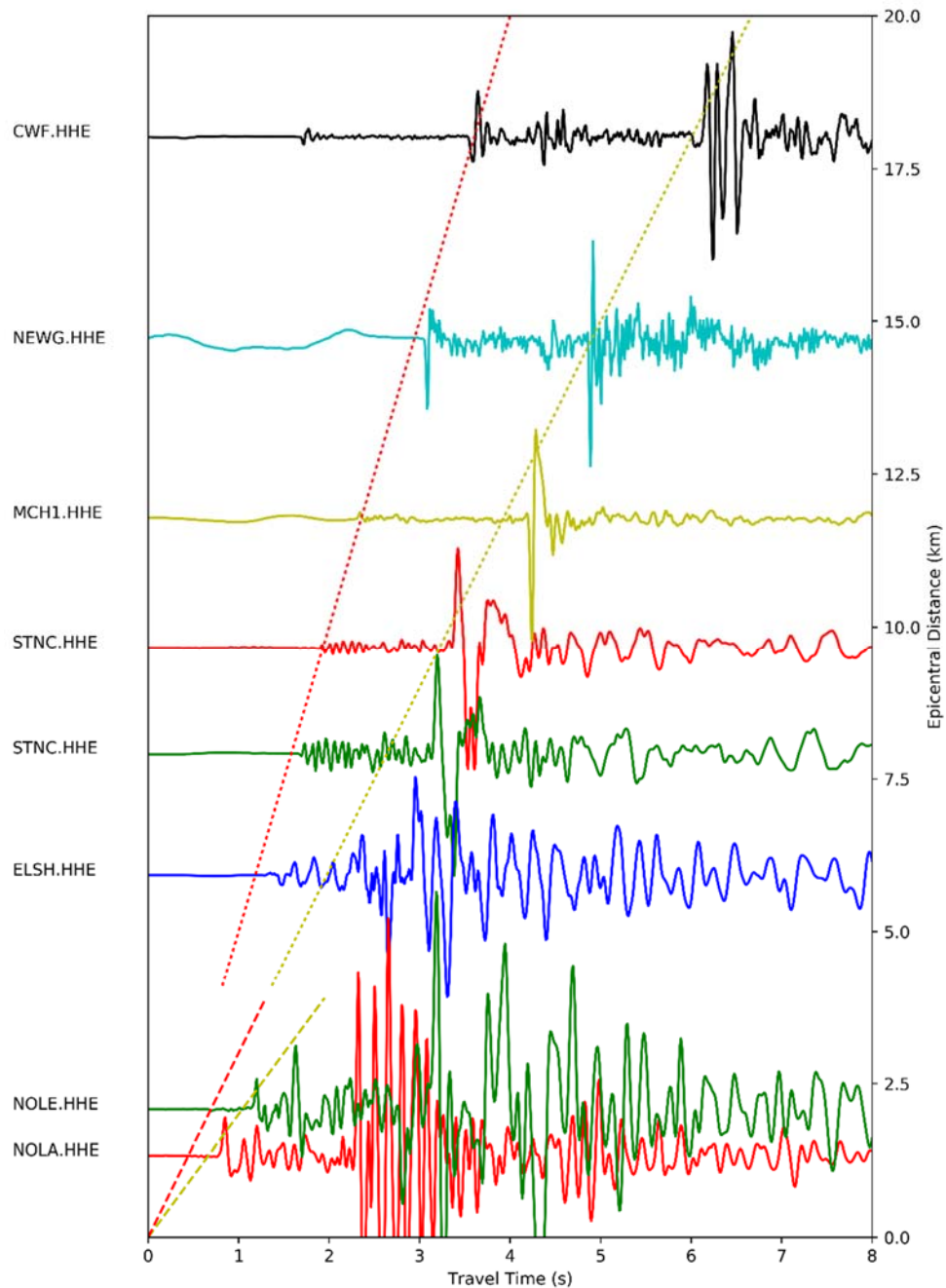
Figure 10. Waveforms at a selection of distances from various earthquakes in the UK dataset. The dotted lines show typical Pg (red) and Sg (yellow) velocities of 5 km/s and 3 km/s. The dashed lines show Pg (red) and Sg (yellow) for shallow crustal paths (3 km/s and 2 km/s). For the stations closer than about 10 km, Sg can be clearly seen but is much smaller than a later arrival (seen at about 2.25 seconds on NOLA and NOLE), which does not have a constant velocity across the traces.
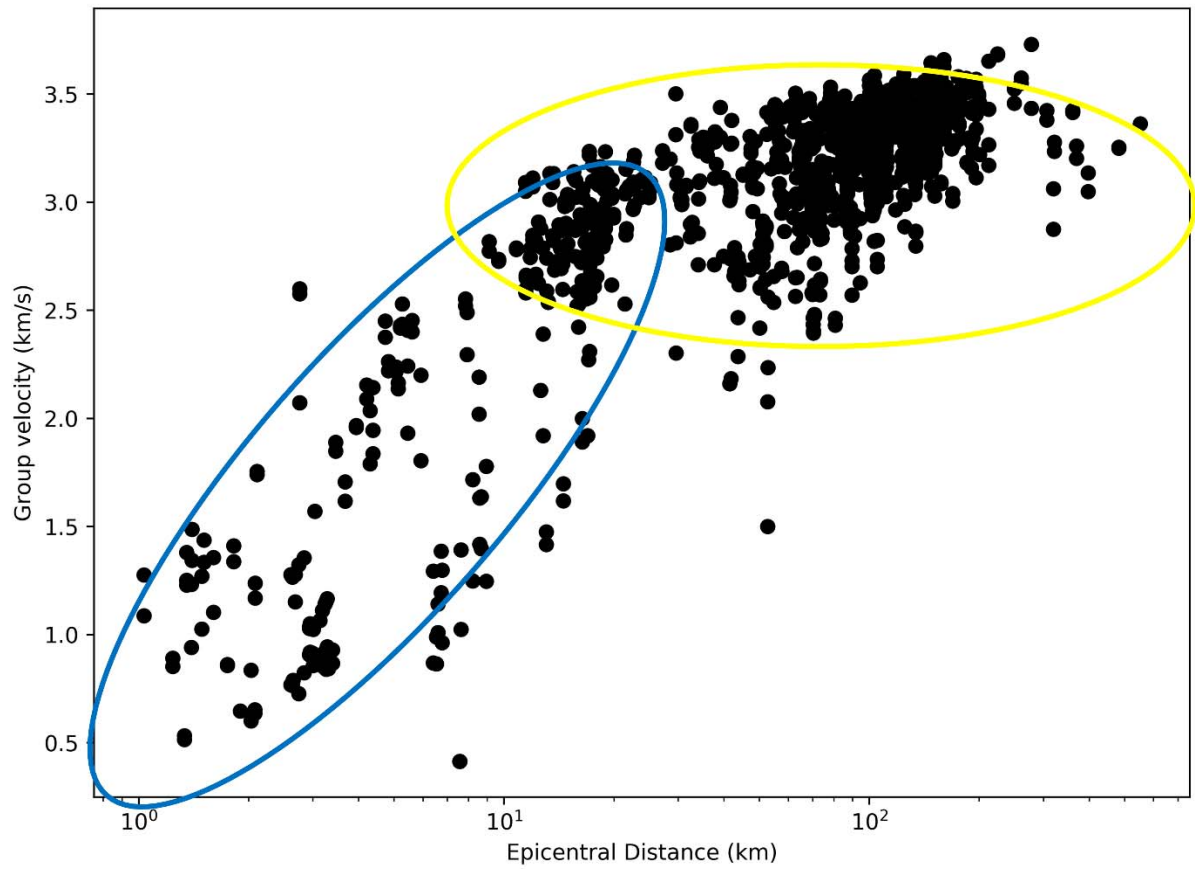
Figure 11. Group velocity for the highest amplitude phase for the UK dataset. Above about 10 km, this is close to 3 km/s as expected for Sg (yellow ellipse) but at shorter distances the velocity increases with distance from the source (blue ellipse).